Development 133, 4737-4748 (2006) doi:10.1242/dev.02658

Grainyhead-related transcription factor is required for duct maturation in the salivary gland and the kidney of the mouse

Yoshifumi Yamaguchi[1,2,*], Shigenobu Yonemura[3] and Shinji Takada[1,4,†]

Duct epithelial structure is an essential feature of many internal organs, including exocrine glands and the kidney. The ducts not only mediate fluid transfer but also help to maintain homeostasis. For instance, fluids and solutes are resorbed from or secreted into the primary fluid flowing through the lumen of the ducts in the exocrine glands and kidneys. The molecular mechanism underlying the functional maturation of these ducts remains largely unknown. Here, we show that a grainyhead-related transcription factor, CP2-like 1 (CP2L1), is required for the maturation of the ducts of the salivary gland and kidney. In the mouse, *Cp2l1* is specifically expressed in the developing ducts of a number of exocrine glands, including the salivary gland, as well as in those of the kidney. In *Cp2l1*-deficient mice, the expression of genes directly involved in functional maturation of the ducts was specifically reduced in both the salivary gland and kidney, indicating that *Cp2l1* is required for the differentiation of duct cells. Furthermore, the composition of saliva and urine was abnormal in these mice. These results indicate that *Cp2l1* expression is required for normal duct development in both the salivary gland and kidney.

KEY WORDS: Grainyhead, Organogenesis, Kidney, Salivary gland

INTRODUCTION

Ducts, which are major epithelial components of tubular organs, mediate the passage and control homeostasis by modifying secretion. The ducts are generated through a series of morphogenetic processes, including epithelial-mesenchymal interaction, branching morphogenesis and lumen formation. Recent studies have revealed that several growth factors, extracellular matrix components and transcriptional factors play important roles in these processes (Davies, 2002; Hogan and Kolodziej, 2002). During the course of morphogenesis, the epithelial cells of the ducts differentiate to acquire their physiological functions; for example, the maintenance of water, mineral and acid-base homeostasis in renal tubules. By contrast to the molecular mechanisms underlying tubule morphogenesis, however, the mechanisms leading to the differentiation of duct epithelial cells remain largely unknown.

Exocrine glands and kidney are typical examples of tubular organs with well-developed ducts. Exocrine glands, including the salivary gland, lachrymal gland and mammary gland, consist of two major epithelial components: a proximal part called the acinus, which generally produces primary fluid by secreting serous fluid into the lumen; and a distal part, the duct, which resorbs or secretes fluids and solutes from or to the primary fluid flowing through its lumen. Thus, in spite of the characteristic and distinct appearance of each exocrine gland, they exhibit similar fundamental structures and functions.

[1]Okazaki Institute for Integrative Biosciences, National Institutes of Natural Sciences, Myodaiji, Okazaki, 444-8787, Japan. [2]Graduate School of Biostudies, Kyoto University, Kitashirakawa, Sakyo-ku, Kyoto, 606-8502, Japan. [3]Laboratory for Cellular Morphogenesis, Center for Developmental Biology, RIKEN, Kobe, 650-0047, Japan. [4]The Graduate University for Advanced Studies (SOKENDAI), Myodaiji, Okazaki, 444-8585, Japan.

*Present address: Department of Genetics, Graduate School of Pharmaceutical Sciences, University of Tokyo, 7-3-1 Hongo, Bunkyo-ku, Tokyo 113-0033, Japan
†Author for correspondence (e-mail: stakada@nibb.ac.jp)

Accepted 22 September 2006

The kidney shares the basic design of these exocrine glands. The kidney processes blood in the proximal part, the glomeruli, to form primary fluid, the primary urine, and then modifies it by absorption and/or secretion of minerals and water in the distal parts, including the ducts and tubules. Therefore, it is thought that a common molecular mechanism underlies the maturation of exocrine glands and the kidney.

Members of the grainyhead gene family of transcriptional factors, which are evolutionarily conserved from *Caenorhabditis elegans* to humans (Venkatesan et al., 2003), have been implicated in the development of epithelial tissues. The molecules of this family exhibit structural similarities in the DNA-binding and oligomerization domains. Six members of this family have been identified in mammals: CP2 (also referred to as UBP-1, LSF, LBP-1c and LBP-1d) (Lim et al., 1992; Yoon et al., 1994), NF2d9 (also referred to as LBP-1a and LBP-1b) (Parekh et al., 2004; Sueyoshi et al., 1995), CP2-like 1 [CP2L1 (TCFCP2L1 – Mouse Genome Informatics); also referred to as CRTR1 in mouse and LBP-9 in humans] (Huang and Miller, 2000; Rodda et al., 2001), mammalian grainyhead [also referred to as LBP-32 and grainyhead-like 1 (GRHL1)], brother of mammalian grainyhead (also known as GRHL2) (Wilanowski et al., 2002) and sister of mammalian grainyhead (also referred to as GET-1 or GRHL3) (Kudryavtseva et al., 2003; Ting et al., 2003). Intriguingly, many, but not all, of the genes of the grainyhead family are expressed in the epithelial tissues and play roles in epithelial morphogenesis and/or homeostasis in a wide variety of animals. For instance, grainyhead-deficient *Drosophila* displays abnormalities in epithelial development and homeostasis, including tracheal development, epidermal cuticle formation and wound healing (Bray and Kafatos, 1991; Hemphala et al., 2003; Mace et al., 2005). Likewise, loss of sister of mammalian grainyhead in mice leads to defects in dorsal epithelial sheet closure and failure in the formation and maintenance of the epidermal barrier (Ting et al., 2005). Inhibition of Grhl1 activity in *Xenopus* results in defective epidermal differentiation (Tao et al., 2005).

As in the case of these grainyhead family genes, *Cp2l1* is also expressed in epithelium in a characteristic pattern: in the developing duct epithelium of the salivary gland and kidney in the mouse embryo (Rodda et al., 2001; Yamaguchi et al., 2005). Interestingly, we found that *Cp2l1* is expressed in the developing epithelial ducts of other organs. Because the ducts of the exocrine glands and the kidney have similar functions, we suspected that CP2L1 plays a role in the developing ducts of these organs. To determine whether this is the case, we examined the precise expression and roles of *Cp2l1* during the development of the salivary gland and the kidney.

MATERIALS AND METHODS

Mouse strains

The production of the *Cp2l1* trap mice has been reported previously (Yamaguchi et al., 2005). These mice were backcrossed into a C57BL/6 background for six to ten generations and then analyzed. Genotypes were determined by PCR amplification using the following primers: a, 5′-CCATAGTGGAGGCCACACGCCCAAGAT-3′; b, 5′-CAAAGGGACCTAAACCACCAGAAGGAGAA-3′; and c, 5′-CTCAGCCTTGAGCCTCTGGAGCTGCTC-3′ (Fig. 1L). Amplification was performed for 35 cycles of 94°C for 30 seconds and 68°C for 30 seconds. The presence of a 725 bp fragment, a 525 bp fragment, or both, indicated animals with tra/tra, +/+, and +/tra genotypes, respectively. Mice carrying the CP2L1 allele in which its exon 2 was flanked by two *loxP* sites were crossed with *Pc36 Cre*-expressing mice (provided by H. Takebayashi) (Ding et al., 2005) to excise exon 2, leading to a frame-shift mutation that generates a null allele of *Cp2l1* (see Fig. S1 in the supplementary material). The complete characterization of these mice will be reported elsewhere.

Chemical analyses of blood, urine, and saliva

Age-matched (4 to 5 months old) wild-type, $Cp2l1^{+/tra}$, and $Cp2l1^{tra/tra}$ male mice were kept in metabolic cages to determine their daily urine output, water intake and urinary electrolyte levels. Plasma samples were collected

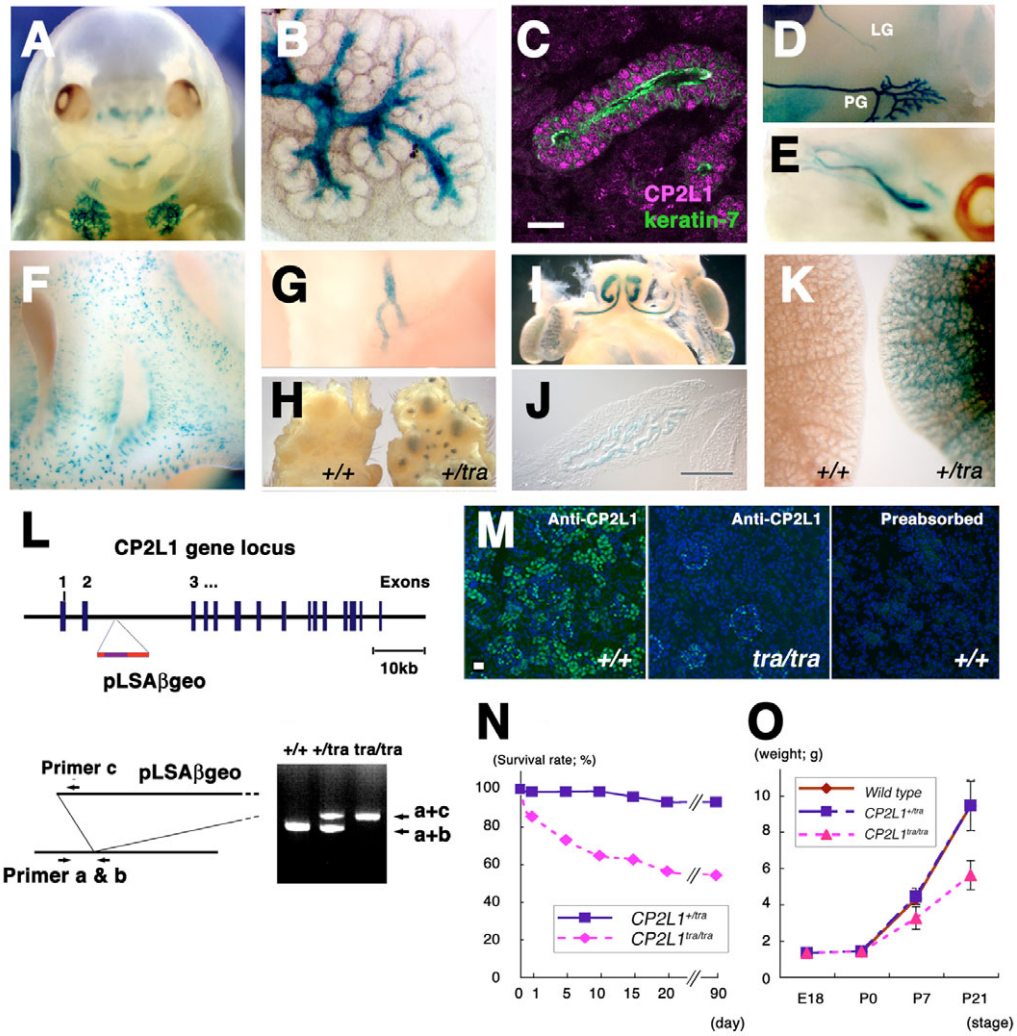

Fig. 1. CP2L1 expression in ducts of exocrine glands and kidney. (A,B,D-K) *LacZ* expression from the *Cp2l1* trap locus in the duct of submandibular and sublingual glands (**A**), isolated SMG (**B**), parotid and lachrymal glands (**D**) and nasal gland (**E**) at E16; in the glandular ducts in olfactory epithelium (**F**) and ducts of the mammary gland (**G**), male reproductive system (**I**), endolymphatic sac (**J**) and lung (**K**; right, $Cp2l1^{+/tra}$; left, wild-type control) at birth; and in eccrine glands in the palm of the adult (**H**; right, $Cp2l1^{+/tra}$; left, wild-type control). (**C**) Co-detection of endogenous CP2L1 protein (magenta) by an antiserum to CP2L1 (As2375) and keratin 7 (green) in the duct of the SMG. (**L**) Genotyping of *Cp2l1* trap locus mice. The gene-trap vector pLSAβgeo was inserted into the second intron of the *Cp2l1* locus. Amplification primers were designed as shown in the lower portion of L. This set of primers could distinguish between the wild-type allele (+) and the *Cp2l1* trap allele (tra). (**M**) Immunohistochemical detection of CP2L1 protein in a kidney section using As2375. Although this serum reacted with unidentified proteins in the cytoplasm of glomerulus cells, CP2L1 protein in the nucleus was not detected in $Cp2l1^{tra/tra}$ mice. (**N**) Survival rate of $Cp2l1^{+/tra}$ (n=56) and $Cp2l1^{tra/tra}$ mice (n=48). (**O**) Growth curve of each genotype. P0-P21, postnatal day 0-21. Scale bar: 25 μm in C,M; 100 μm in J. LG, lachrymal glands; PG, parotid glands.

Table 1. Primers used for cloning of cDNAs

Gene	Forward primer	Reverse primer
Fxyd2b	CGTACCTCAGACACCTCCAG	TTGACCTGCCTATGTTTCTT
Fxyd2c	CAAGGCCAGGTGTGAGTGCT	GCATCGAACTTCAGGCTCCA
Scnn1b	AATGGAACTGTGTGTACCTTGCG	TGGGGATCTAGATGGCCTCCACC
Slc34a1	GTGGGGGATGAGTCCCTGAGGA	GGCATTGTGGTGAGCAGGCAGT
Slc4a1	TGATGGGGGTGTCGGAGCTG	AGGCCACACAGCCAGCAGGA

from the tail artery. For saliva collection, mice were anesthetized by intraperitoneal administration of Nembutal. Pilocarpine hydrochloride (Sigma) was dissolved in distilled water and injected intraperitoneally (2 μg/g body weight) to stimulate saliva production. Immediately after the injection of pilocarpine, saliva was collected in three 5 minute intervals with 100 μl microcapillary pipettes. The volume of saliva secretion was determined and normalized by body weight. Electrolyte levels were measured using a DriChem® multilayer film analyzer (Fuji Film).

Histology and electron microscopy

Organs were fixed in Bouin's fixatives or 4% paraformaldehyde (PFA), dehydrated, embedded in paraffin and sliced into 6 μm sections. The sections were stained with hematoxylin and eosin or Periodic acid/Schiff (PAS) reaction according to standard procedures. For electron microscopic observation, organs were cut and fixed in 2.5% glutaraldehyde and 2% formaldehyde in 0.1 mol/l cacodylate buffer (pH 7.2) and then processed for thin sectioning and transmission electron microscopy.

Immunofluorescence

Cryosections (10 μm) were fixed in 4% PFA and then stained with antibodies specific to aquaporin 2 (AQP2; gift from S. Sasaki), keratin 7 (Dako), pan-cytokeratin (Sigma) or a rabbit antiserum (As2375) raised against the N-terminal 19 amino acids of CP2L1 (NH_2-MLFWHTQPEHYNQHNSGSC-COOH) conjugated to Keyhole Limpet Hemocyanin. For the staining of keratin 7, sections were heated for 10 minutes in a microwave in 10 mmol/l Tris-HCl (pH 9.5) containing 1 mmol/l EDTA. Secondary antibodies conjugated to Cy3 (Jackson ImmunoResearch) or Alexa Fluor 488 (Molecular Probes) were used. Photomicrographs were obtained with a Zeiss Axiophot2 photomicroscope or with a Zeiss LSM510.

Dissection of nephrons

To visualize the nephron segment, kidneys were dissociated and cultured for 12 hours with mesenchyme. Briefly, embryonic day (E) 14 to 16 kidneys were isolated from embryos, incubated in 2% pancreatin (Sigma) for 2 to 5 minutes on ice, and washed three times with Dulbecco's modified Eagle's medium (DMEM) containing 20% fetal bovine serum. The kidneys were then dissociated by pipetting vigorously for 50 times using a Gilson pipetman with 200 μl tip. After this treatment, the samples were seeded on gelatin-coated dishes, cultured for 12 hours in DMEM containing 10% fetal bovine serum and then processed for X-gal staining. In this culture system, dissociated mesenchyme serves as a feeder layer for the undissociated nephrons.

X-gal staining and in situ hybridization

X-gal staining was performed as described previously (Yamaguchi et al., 2005). Briefly, fresh cryosections were fixed in 1% formaldehyde or 2% PFA for 5 to 10 minutes, washed twice with phosphate-buffered saline, and stained for *lacZ* activity. For whole-mount visualization, post-fixed stained embryos were incubated in 1% KOH overnight and gently shaken in distilled water until the embryos became transparent. In situ hybridization on cryosections (10 μm thickness) was performed as previously described (Muroyama et al., 2002). X-gal-stained sections were fixed with 4% PFA for 10 minutes and then processed for in situ hybridization. The following template cDNA plasmids were used for the synthesis of probes: keratin 7 (IMAGE clones 354520); *Gk-6* (IMAGE clones 581222); keratin 19 (IMAGE clones 3164228); *Atp6b1* (IMAGE clones 4489144); *Clcnkb* (IMAGE clones 4975792); *Umod*, *Nkcc2*, *Ncc* and *Ncx* (gifts from S. Nakai) (Nakai et al., 2003); *Cp2l1* (Yamaguchi et al., 2005); *Pax2* (gift from P. Gruss); and *β-NGF, Sgn1* and *Mist1* (gifts from S. Yoshida) (Yoshida et al., 2001). The cDNAs of *Fxyd2 variant b*, *Fxyd2 variant c*, *Scnn1b, Slc34a1* and *Slc4a1* were cloned by PCR using the primers described in Table 1. INT/BCIP (Roche) solution was used as a substrate for signal detection of in situ hybridization after X-gal staining. Nuclear Fast Red (Ventana) was used for counterstaining.

Organ culture

Kidneys were isolated from E13 or E14 embryos, and cultured in DMEM/F12 supplemented with 150 μg/ml vitamin C and 50 μg/ml transferrin on polycarbonate membrane filter (Transwell®, Corning). After 2 days, the explants were processed for RNA extraction.

Quantitative RT-PCR

Quantitative RT-PCR was performed using a LightCycler thermal cycler (Roche). Total RNA was extracted from the kidneys and submandibular glands (SMGs) of embryos and newborn mice using TRIZOL reagent

Table 2. Primers used for quantitative RT-PCR

Gene	Forward primer	Reverse primer	PCR product size (bp)
Podxl	GCCAAGCAACCCTACACCATTC	TCGCTGTGCTCGGTGAAGAATC	358
Slc34a1	AGCAGCTCCGTGTTCACCTC	GCAGCGGGTACCACAGTAGG	222
Umod	TGGTACTGTGAGTGCTCCC	TGTGGACCACCGGCAGCAT	350
Nkcc2	TTTCAATGGCTTCACTTCTCAGC	CGAACTTGACGGTAACTCTT	243
Nos1	AGCATCACCCCTGTCTTCCA	CTTGGGATTTGCCTGTCTCG	246
Ncc	AGATGAGACAGGCACCAACA	CAGTAGGTCCCTTACGGTTT	381
Ncx1	AAGAAACCGAATGGAGAGACC	TAAGCAAGCCTTCCCAGACC	366
Gk-6	CCCACAACCTGAGGATGACT	CATTAGGCAGGAGCTTGAGG	214
Fxyd2b	CGTACCTCAGACACCTCCAG	TTGACCTGCCTATGTTTCTT	209
Fxyd2C	CGGGGTTTGGGACTTCTAGC	GGGATTCTCTGTCCCCTTGG	299
Aqp2	ACCTGGGTAGCCCTGCTCTC	CCGATCCAGAAGACCCAGTG	153
Scnn1b	GTGCCACCCAGGCCGTAACT	GCCCCTGCTGTGGACGC	318
keratin 7	CAGGCAGAGATTGACACCTT	GCGCCAGCTTGGTGTTCAG	198
keratin 19	GGTGTCGACCTAGCCAAGA	TCTCTGCCAGCGTGCCTT	255
Hprt	GCTGGTGAAAAGGACCTCT	CACAGGACTAGAACACCTGC	248
Clcnkb	TACACTGGCCAAGGACATGC	AGGAAGCTGGCTCAGTCTGG	160
Atp6b1	TCAATCCCCATGACCGAATC	CCAGCACAGCCTTGGATTTC	188
cyclophilin D	GCAAGGATGGCAAGGATTGA	AGCAATTCTGCCTGGATAGC	91
pendrin	CATCGATGGGAACCAGGAAT	TGGCAACCATCACAATCACA	169

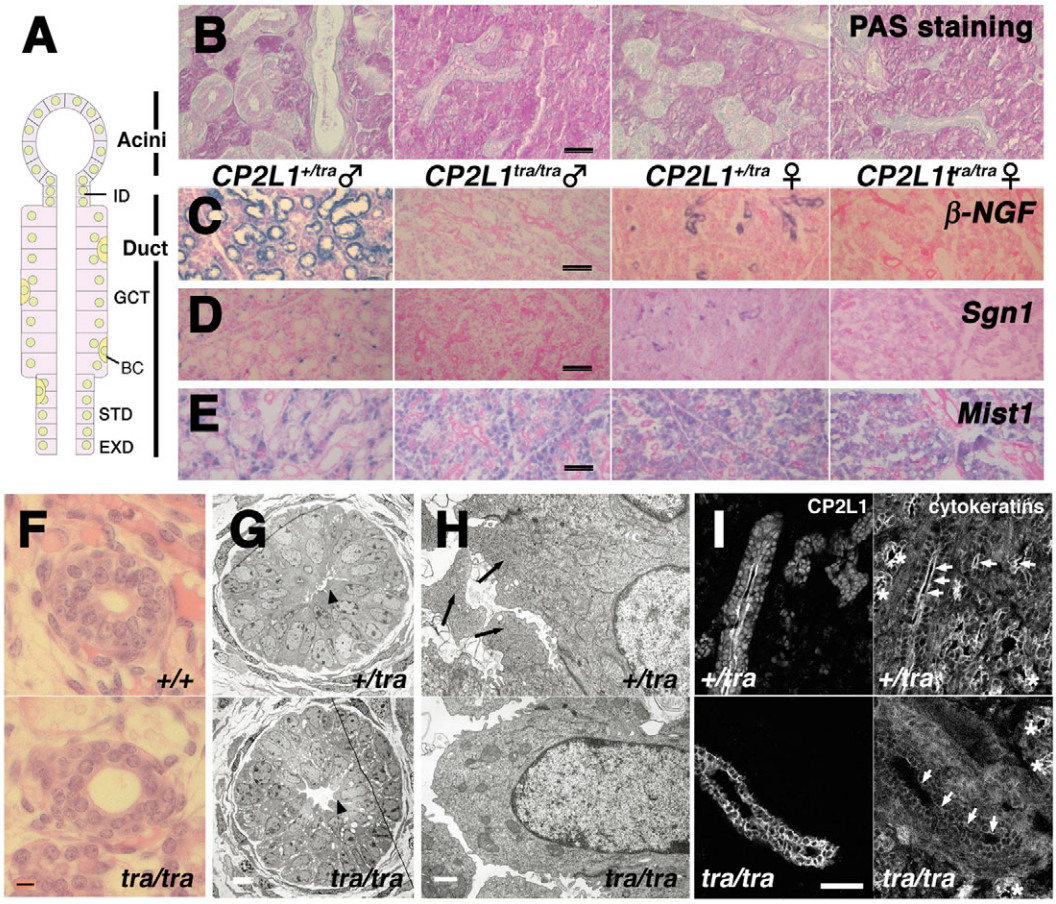

Fig. 2. Morphological abnormality in the submandibular duct of *Cp2l1*$^{tra/tra}$ mice. (**A**) Schematic representation of the rodent SMG. (**B**) Morphological abnormalities observed in adult male and female *Cp2l1*$^{tra/tra}$ mice. (**C-E**) In situ hybridization analysis of the adult SMG. Nuclei were counterstained with nuclear Fast Red (red). The GCT marker *β-NGF* (C) and the basal cell marker *Sgn1* (D) were not detected in either male or female *Cp2l1*$^{tra/tra}$ mice. *Mist1* expression was normal in the mutants (E). (**F**) Hematoxylin/eosin-stained sections of wild-type (+/+) and *Cp2l1*$^{tra/tra}$ (tra/tra) fetuses at E18. Although the numbers of cells surrounding the lumen of *Cp2l1*$^{tra/tra}$ was almost equal to that of *Cp2l1*$^{+/tra}$ mice [mean cell number ± standard deviation, 9.0±1.7 (n=25) versus 8.8±1.8 (n=20) in intralobular ducts and 10.8±1.7 (n=20) versus 10.2±1.8 (n=16) in the excretory ducts], the lumen of *Cp2l1*$^{tra/tra}$ was significantly wider in *Cp2l1*$^{+/tra}$ than in *Cp2l1*$^{tra/tra}$ mice [mean diameter ± standard deviation, 2.69±0.83 (n=25) versus 3.68±1.16 μm (n=20) in the intralobular ducts (P<0.005) and 5.34±2.77 (n=20) and 7.2±2.0 μm (n=16) in the excretory ducts (P<0.05)]. (**G**,**H**) Electron microscopic observations of the duct. Apical structures of luminal cells (arrowheads in G and arrows in H) did not develop sufficiently in *Cp2l1*$^{tra/tra}$ compared with *Cp2l1*$^{+/tra}$ mice. (**I**) Immunohistological staining of CP2L1 and keratins in the SMG at birth. Anti-CP2L1 immunoreactivity was found only in the duct cells (left panels). Detection of cytokeratins (right panels) on the luminal surface in both the ducts (white arrows) and acini (asterisks) in *Cp2l1*$^{+/tra}$ mice. In *Cp2l1*$^{tra/tra}$ mice, cytokeratins were detected in acini but not in the ducts. Scale bars: 100 μm in B-E; 10 μm in F; 7 μm in G; 1 μm in H; 50 μm in I. BC, basal cell; EXD, excretory duct; ID, intercalated duct; STD, striated duct.

(Invitrogen) and then purified using the RNeasy total RNA purification kit (Qiagen). Following treatment with DNaseI, cDNA was generated from 2 μg of total RNA using SuperScriptIII reverse transcriptase (Invitrogen) and a random hexamer in a total volume of 20 μl. PCR was then carried out using SYBR Green Premix Ex Taq (Takara) and gene-specific primers (Table 2). At least four samples per genotype or stage were quantified, and the expression level of each gene was normalized with that of hypoxanthine guanine phosphoribosyl transferase (HPRT) or cyclophilin D1 (identical results were obtained with both). Differences were analyzed using Student's t-test.

RESULTS

Cp2l1 expression in fluid/solute-transporting epithelial tissues

During the course of gene-trap mutagenesis (Yamaguchi et al., 2005), we found that *Cp2l1* is expressed in the epithelium of the developing salivary (submandibular, sublingual and parotid) glands (Fig. 1A-D) and kidney (Fig. 4) (Yamaguchi et al., 2005). More extensive and sensitive analysis of expression by in situ hybridization and *lacZ* staining revealed that this gene was also expressed in the ducts of other exocrine glands, including the lachrymal glands (Fig. 1D), nasal glands (Fig. 1E), minor nasal glands in the olfactory epithelium (Fig. 1F), mammary glands (Fig. 1G) and eccrine sweat glands (Fig. 1H). However, we did not detect expression of *Cp2l1* during the development of the pancreas, which is an exocrine gland. In addition to exocrine glands, *Cp2l1* was also expressed during development of other epithelial tissues, including the ductus epididymis, ductus deferens and seminal vesicles (Fig. 1I). We also detected expression of *Cp2l1* at birth in the endolymphatic sac in the inner ear (Fig. 1J), lung (Fig. 1K), thyroid gland and meninx (data not shown). Thus, the expression of *Cp2l1* is mainly associated with epithelial structures in which fluids and solutes are actively transported.

Submandibular ducts are defective in *Cp2l1*$^{tra/tra}$ mice

We previously generated mice homozygous for a gene-trap insertion in the *Cp2l1* locus (*Cp2l1*^{tra}) (Fig. 1L). These mutant mice express little mRNA for the full-length CP2L1 protein. Instead, they express a truncated form that contains only the N-terminal portion and lacks the DNA-binding domain (Yamaguchi et al., 2005). This truncated protein did not appear to be localized in the nucleus because we detected membrane or cytosolic but not nuclear staining for CP2L1 in the submandibular duct of *Cp2l1*$^{tra/tra}$ mice (Fig. 2I; left panels). Furthermore, expression of the truncated protein was below the

detectable level in the kidney of *Cp2l1*$^{tra/tra}$ mice, although the anti-CP2L1 antibody used in this study reacted with unidentified proteins in the cytoplasm of glomerulus cells, which do not express *Cp2l1* mRNA (Fig. 1M). Thus, we concluded that the truncated CP2L1 produced in these mice mostly lacks the ability to function as a transcription factor. We also found that mice homozygous for the *Cp2l1* null locus generated separately by a gene-targeting strategy exhibit the same phenotype as the *Cp2l1*$^{tra/tra}$ mice (see Fig. S1 in the supplementary material). We then used the trapped allele for further analysis of CP2L1 function. Intercrossing within the heterozygotes resulted in homozygous mice with nearly the expected Mendelian distribution (*Cp2l1*$^{+/+}$: *Cp2l1*$^{+/tra}$: *Cp2l1*$^{tra/tra}$=49:73:45). Approximately half these mice died before weaning and showed growth retardation during early postnatal stages, although mutant mice that survived past weaning recovered to 80-90% of the weight of the wild-type mice (Fig. 1N,O and data not shown).

To address whether CP2L1 is required for the development of ducts, we first investigated the salivary glands in surviving adult *Cp2l1*$^{tra/tra}$ mice. Mammals have three major salivary glands, the submandibular, sublingual and parotid glands, which are formed through similar developmental processes. The patterns of *Cp2l1* expression in these glands during development and in adults were similar. Because the submandibular gland (SMG) is the most prominent structure, we mainly focused on it. The SMG of rodents contains several types of ducts distinguished by their location and morphological appearance: namely, intercalated duct, striated duct, excretory duct and granular convoluted tubule (GCT) (Fig. 2A) (Tandler, 1993). Maturation of the GCTs occurs under the control of androgen and thyroxine after birth (Gresik and Barka, 1980), and there is sexual dimorphism in this process; in the GCT, the volume of cytoplasm was greater in males than in females (Fig. 2B; see Fig. S1D in the supplementary material). By contrast to *Cp2l1*$^{+/+}$ and *Cp2l1*$^{+/tra}$ mice, the *Cp2l1*$^{tra/tra}$ mice exhibited defects in the morphology of the ducts; duct structure was not well developed, and the volume of cytoplasm in the duct epithelial cells was reduced (Fig. 2B). In particular, we did not observe cell shapes characteristic of striated and excretory ducts and GCT. Consistent with this observation, we found that the expression of *β-NGF* (*Ngfb* – Mouse Genome Informatics) and glandular kallikrein 6 (*Gk-6*; *Klk1* – Mouse Genome Informatics), which is increased according to the maturation of GCTs (Penschow et al., 1991; Yoshida et al., 2001), was diminished in both male and female *Cp2l1*$^{tra/tra}$ mice (Fig. 2C and data not shown). In addition, we did not detect the expression of *Sgn1* (also known as *Ascl3* – Mouse Genome Informatics) in basal cells (Yoshida et al., 2001) of the salivary duct in *Cp2l1*$^{tra/tra}$ mice (Fig. 2D). By contrast, morphological observation and analysis of *Mist1* (*Bhlhb8* – Mouse Genome Informatics), an acinus-specific basic helix-loop-helix transcriptional factor (Yoshida et al., 2001), indicated that there were no obvious abnormalities in the acini of either male or female *Cp2l1*$^{tra/tra}$ mice, a portion of exocrine gland that does not express CP2L1 in normal mice (Fig. 2E). These results indicated that the duct epithelial cells did not mature properly in the SMG of *Cp2l1*$^{tra/tra}$ mice.

Defective maturation of the salivary gland in *Cp2l1*$^{tra/tra}$ embryos

We next examined the onset of the abnormalities during the development of *Cp2l1*$^{tra/tra}$ embryos. During the development of the salivary glands, *Cp2l1* is first expressed at E12.5 in the stalk

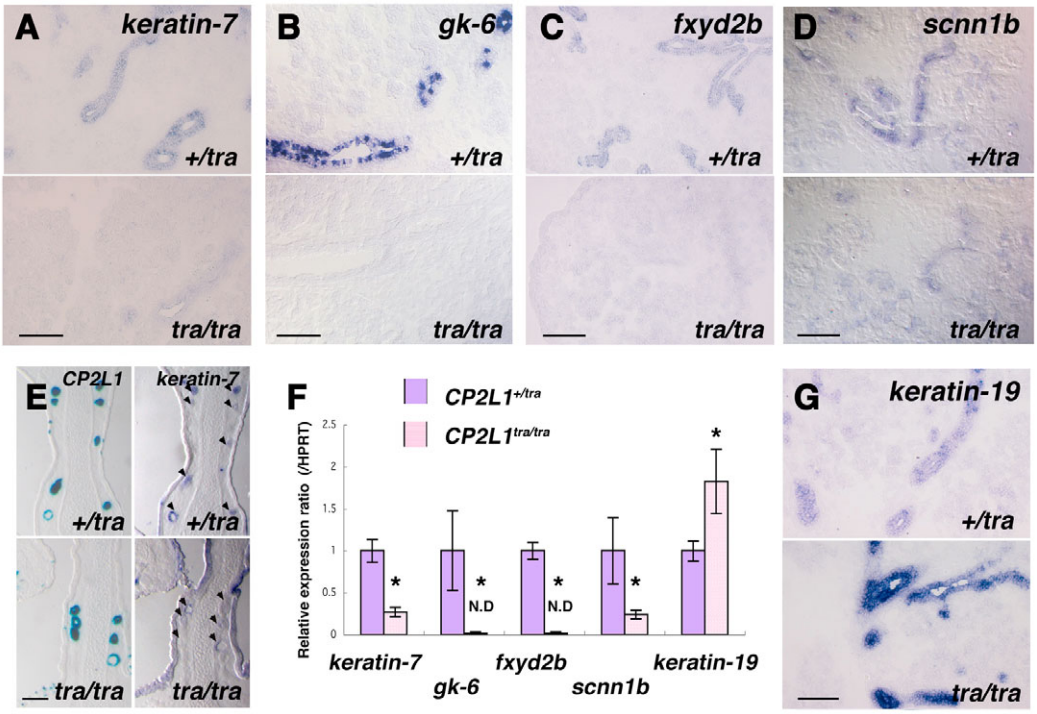

Fig. 3. Abnormalities in gene expression in the SMG of *Cp2l1*$^{tra/tra}$ mice. (**A-D**,**G**) In situ hybridization analysis of the SMG at birth. Expression of the duct-specific genes keratin 7 (A), *Gk-6* (B), *Fxyd2b* (C), *Scnn1b* (D) and keratin 19 (G) was abnormal in *Cp2l1*$^{tra/tra}$ mice compared with *Cp2l1*$^{+/tra}$ mice. (**E**) Expression of CP2L1 and keratin 7 examined in adjacent sections of the nasal gland. In the duct of the nasal gland, *Cp2l1* (*lacZ* expression; left) was coexpressed with keratin 7 (right) in control *Cp2l1*$^{+/tra}$ mice (upper panels). In *Cp2l1*$^{tra/tra}$ mice (lower panels), based on the morphology and the expression of *Cp2l1* (left), the duct was formed, although keratin 7 (right) was not expressed. (**F**) Comparison of mRNA expression levels in the newborn SMG of *Cp2l1*$^{+/tra}$ and *Cp2l1*$^{tra/tra}$ mice by quantitative RT-PCR. *P<0.005. Scale bars: 100 μm.

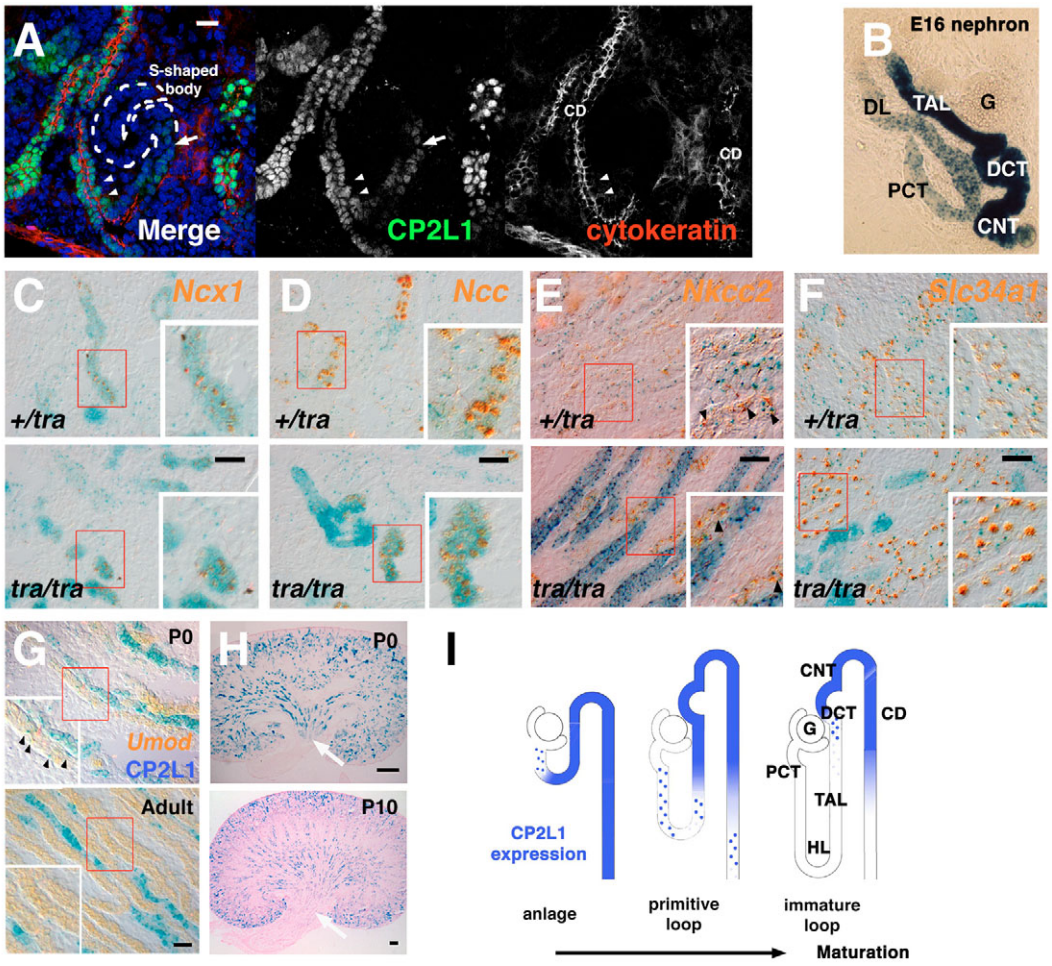

Fig. 4. CP2L1 expression during kidney development. (**A**) Detection of CP2L1 protein (green) in the ureteric epithelium (CD; arrowhead), identified by expression of cytokeratin (red), and at the distal end of the S-shaped body (arrow) at birth. DNA was stained with TOPRO3 (blue). (**B**) CP2L1 (*lacZ*) was detected strongly in the CNT, DCT and TAL and weakly in the DL and PCT at the primitive loop nephron at E16. (**C-F**) Identification of CP2L1 expression domains at birth by co-labeling by *LacZ* staining (blue) and in situ hybridization (orange). Insets: higher magnification of boxed regions. CP2L1 (*LacZ*) was strongly coexpressed with *Ncx1* (C) and modestly or weakly with *Ncc* (D) at the immature loop nephron in deeper regions of the cortex. Few CP2L1 were detected with *Nkcc2* (E) (arrowheads) and *Slc34a1* (F). Note that RNA localization of several genes, including *Slc34a1, Ncx1* and *Ncc* (C,D,F), was detected only in the nucleus by in situ hybridization used in this analysis. (**G**) Double-labeling of CP2L1 (*lacZ*) and *Umod* (orange) in the medulla. The expression of CP2L1 was weakly detected in *Umod*-positive TAL at P0 (blue dots indicated by black arrowheads in the upper inset) but disappeared in adulthood. (**H**) Expression of CP2L1 (*lacZ*) at P0 and P10. The expression was lost at P10 in the papillary region (white arrows). (**I**) Summary of CP2L1 expression. The expression shifts during the course of nephron maturation. Scale bar: 20 μm in A; 50 μm in C-G; 200 μm in H.

and subsequently in the cells of the ducts (Yamaguchi et al., 2005). In *Cp2l1*$^{tra/tra}$ embryos, the SMG did not exhibit obvious morphological abnormalities until E16 (data not shown). At E18, however, luminal cells in the SMG ducts of *Cp2l1*$^{tra/tra}$ embryos were shorter in the apico-basal direction than those of *Cp2l1*$^{+/+}$ and *Cp2l1*$^{+/tra}$ mice (Fig. 2F). Consistent with this abnormal cell shape, the lumen of the SMG ducts was noticeably wider in the mutant embryos. Formation of adherens and tight junctions in the duct appeared to be normal, because the localization of E-cadherin and ZO-1 were normal (data not shown). Electron microscopic analysis, however, revealed that the apical structure of the luminal cells in normal embryos did not develop sufficiently in the mutant embryos (Fig. 2G,H). In agreement with this observation, cytokeratin proteins were not detected in the apical side of the luminal cells in the ducts of mutants (shown by white arrows in the right panels of Fig. 2I). Except for the lumens of the ducts, *Cp2l1* expression was not detected in the lobule or primodium of acini, and the morphology and cytokeratin localization were normal in the acini of *Cp2l1*$^{tra/tra}$ embryos (shown by asterisks in the right panels of Fig. 2I), suggesting a specific defect in the development of salivary gland duct cells in *Cp2l1*$^{tra/tra}$ embryos.

The morphological abnormality observed in *Cp2l1*$^{tra/tra}$ embryos was accompanied by abnormal gene expression. Keratin 7, a type 2 basic intermediate filament, is expressed strongly in the ducts of many glandular tissues and kidney (Fig. 1C) (Smith et al., 2002). Although keratin 7 mRNA was detected from E14 in the duct of the SMG in normal embryos, its expression was obviously reduced throughout development in *Cp2l1*$^{tra/tra}$ embryos (Fig. 3A and data not shown). In addition, some other genes also failed to be expressed in the SMG duct of *Cp2l1*$^{tra/tra}$ mice. The expression of *Gk-6* (Penschow et al., 1991), *Fxyd2a* and *Fxyd2b* (genes encoding Na^+,K^+-ATPase γ-subunit variants a and b) (Jones et al., 2001; Jones et al., 2005), and *Scnn1b* (gene encoding the β-subunit of the epithelial sodium channel) in the SMG was detected during normal development but severely reduced in *Cp2l1*$^{tra/tra}$ embryos throughout development (Fig. 3B-D,F and data not shown). These results indicate that, despite formation of the duct structure, the cells constituting the duct failed to differentiate properly in *Cp2l1*$^{tra/tra}$ embryos. In addition, these genes were not properly expressed in the ducts of the sublingual or the parotid gland of *Cp2l1*$^{tra/tra}$ embryos, indicating that CP2L1 plays similar roles in the maturation of major ducts in the salivary glands (data not shown). In addition to the salivary glands, we observed expression

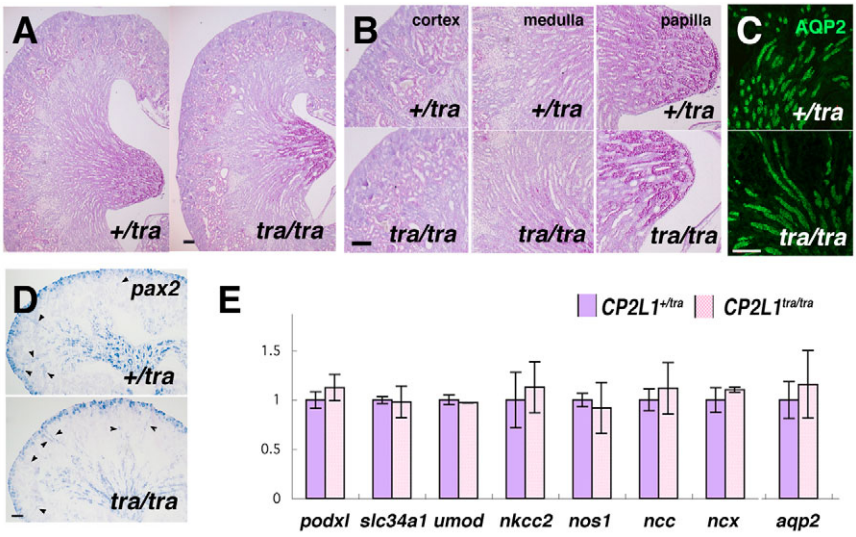

Fig. 5. Kidney formation in *Cp2l1*$^{tra/tra}$ mice. (**A**,**B**) PAS staining of a kidney section at postnatal day 2. Higher magnification figures of A are shown in B. (**C**) Expression of AQP2 protein in the medulla was normal in both newborn *Cp2l1*$^{+/tra}$ and *Cp2l1*$^{tra/tra}$ mice. (**D**) Expression of *Pax2* in CD (arrowheads) was normal even in *Cp2l1*$^{tra/tra}$ mice at birth. (**E**) Quantification of mRNA expression levels of nephron segmental marker genes at birth by quantitative RT-PCR. Values represent mean expression levels ± standard deviation (n=4-9). The experiments were repeated at least twice, and there was no significant difference between *Cp2l1*$^{+/tra}$ and *Cp2l1*$^{tra/tra}$ mice. Scale bars: 200 μm.

of keratin 7 and *Gk-6* in the duct of the nasal gland, and their expression was also lost in *Cp2l1*$^{tra/tra}$ embryos (Fig. 3E and data not shown). Thus, CP2L1 appears to play similar roles in different exocrine glands.

However, the expression of keratin 19 was increased in the duct of *Cp2l1*$^{tra/tra}$ mice at birth (Fig. 3F,G). To better understand the temporal expression pattern of this gene, we profiled its normal expression. We found that, until birth, keratin 19 is expressed in the duct and the stalk, which is an immature form of the duct, but that its expression is gradually reduced in the distal (oral cavity side) to proximal (acinus side) direction (data not shown). Thus, elevated expression of keratin 19 in *Cp2l1*$^{tra/tra}$ newborn mice probably reflects an undifferentiated state of duct epithelial cells. Taken together, these results clearly indicate that CP2L1 is required for proper maturation of the submandibular duct.

Expression of *Cp2l1* during kidney development

Our preliminary analysis indicated that the kidney is developed in *Cp2l1*$^{tra/tra}$ mice but with occasional hypoplasia (Yamaguchi et al., 2005). In the current studies, we first performed a precise analysis of *Cp2l1* expression during kidney development. The kidney consists of numerous nephrons and collecting duct (CD) systems. A secretory nephron consists of Bowman's capsule, which filters blood to form the primary urine, and a tubule, which is subdivided into several compartments: the proximal convoluted tubule (PCT); the descending limb (DL); the thick ascending limb (TAL); and a distal tubule, which is made up of the distal convoluted tubule (DCT) and the connecting tubule (CNT), arranged in the order of primary urine flow. A secretory nephron is connected to the CD by the CNT (Fig. 4I).

CP2L1 was expressed both in CD lineages and nephrons. During renal development, CP2L1 is first expressed in the nephric duct and subsequently in the branching ureteric epithelium, which differentiates into the CD (Yamaguchi et al., 2005). CP2L1 expression was subsequently observed in CD cells, which are characterized by expression of cytokeratin and AQP2 (Fig. 4A and data not shown), and later localized to the medullary and cortical, but not papillary, CDs (Fig. 4H,I). In the nephron, expression of CP2L1 (*lacZ* expression from the trapped CP2L1 allele) was first detected in a distal region of S-shaped bodies, which differentiates into the tubular portion of the nephron (Fig. 4A; arrowhead) (Yamaguchi et al., 2005). After the S-shaped body stage, the nephron maturates through four sequential stages characterized by development of the loop of Henle (HL, consisting of DL and TAL): the anlage, the primitive loop, the immature loop and the mature loop (Fig. 4I) (Neiss, 1982; Nakai et al., 2003), and nephrogenesis continues repetitiously in the peripheral region of the kidney until around P10, resulting in a large number of nephrons in a kidney. At the anlage stage, CP2L1 expression was detected in all nephric tubule (data not shown). Then, at the primitive loop stage, CP2L1 was expressed strongly in the distal portion (TAL, DCT and CNT) and weakly in the proximal portion (DL and PCT) but not in the glomerulus (Fig. 4B). At the immature loop stage, strong expression of CP2L1 was observed in cells expressing Ncx1 (Slc8a1 – Mouse Genome Informatics) (Na^+/Ca^{2+} exchanger 1; Fig. 4C), a marker for CNT. Modest or low expression was colocalized with expression of the DCT marker, Ncc (Slc12a3 – Mouse Genome Informatics) (Na^+/Cl^- co-transporter; Fig. 4D). We observed very weak expression in the form of a faint dot in more proximal regions of the nephron along with expression of Nkcc2 (Slc12a1 – Mouse Genome Informatics), Umod and Slc34a1 (Fig. 4E-G), which are specific for TAL, HL and PCT, respectively (Grieshammer et al., 2005; Nakai et al., 2003). At the mature loop stage (adult kidney), CP2L1 was no longer expressed in the TAL (Fig. 4G, lower panel), and it was detected weakly in the CNT, and a part of the DCT (data not shown). Thus, during the maturation of the kidney, CP2L1 expression is localized to more distal regions in the nephron (Fig. 4I).

Defective maturation in distal nephric tubules and the collecting duct in the kidney of *Cp2l1*$^{tra/tra}$ mice

We next examined the kidney phenotype of *Cp2l1*$^{tra/tra}$ mice. Because *Cp2l1*$^{tra/tra}$ mice often died within 2 days after birth (Fig. 1N), we first examined the mutant kidney around birth. Obvious structural abnormalities were not apparent at this time in the kidney of *Cp2l1*$^{tra/tra}$ mice (Fig. 5A,B). To examine whether the nephron and CD were properly formed, we used in situ hybridization and quantitative RT-PCR to examine the expression of a series of genes specific to distinct portions of the renal tubule in *Cp2l1*$^{tra/tra}$ mice. We found normal expression at E18 and birth in the nephron of *Cp2l1*$^{tra/tra}$ mice for the following marker genes: *Podxl*, a marker for glomeruli; *Slc34a1* for PCT; *Umod* for Henle's loop; *Nkcc2* for TAL; *Nos1* for macula densa; *Ncc* for DCT; and *Ncx1* for CNT (Fig. 4C-F, Fig. 5E and data not shown) (Grieshammer et al., 2005; Nakai et al., 2003). The expression of two CD markers, *Aqp2* and *Pax2*, was also

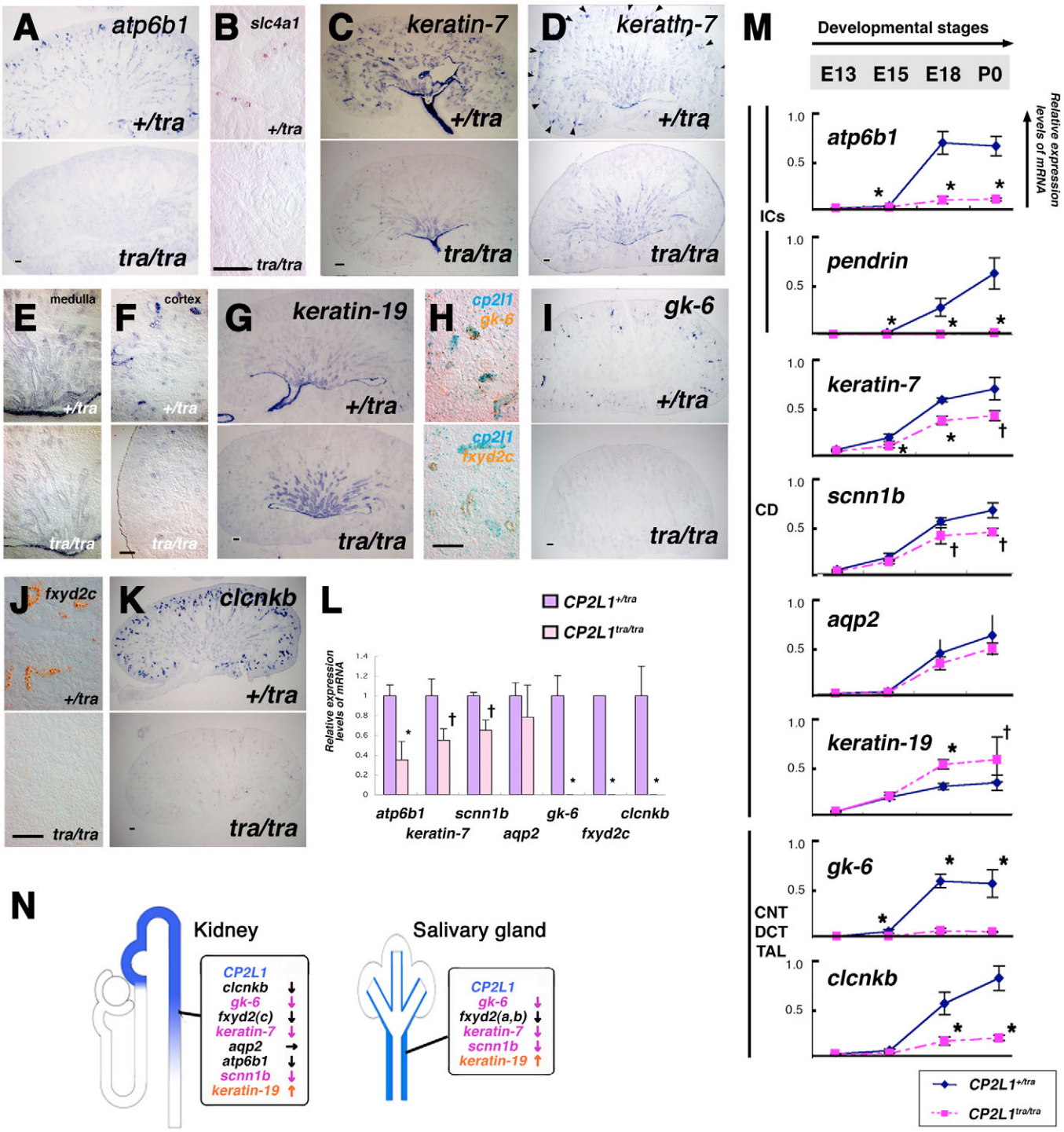

Fig. 6. Differentiation defects in the kidney of *Cp2l1*$^{tra/tra}$ mice. (**A-K**) In situ hybridization analysis of the kidney at birth. Expression of IC markers *Atp6b1* (A) and *Slc4a1* (B) was lost in *Cp2l1*$^{tra/tra}$ mice. Expression of keratin 7 was lower in the whole CD of *Cp2l1*$^{tra/tra}$ mice at E18 (C,E) and in the cortical CD (D,F; arrowheads) of newborn *Cp2l1*$^{tra/tra}$ mice. By contrast, keratin 19 was more strongly expressed in the inner medullary CD of *Cp2l1*$^{tra/tra}$ mice than *Cp2l1*$^{+/tra}$ mice at birth (G). Expression of *Gk-6* and *Fxyd2c* (orange) in DCT and CNT overlapped with that of *Cp2l1* (*lacZ* staining; blue) (H). Expression of *Gk-6* and *Fxyd2c* was not detected in *Cp2l1*$^{tra/tra}$ mice at E18 (I,J). Expression of *Clcnkb* was also absent in the distal tubules of *Cp2l1*$^{tra/tra}$ mice (K). (**L**,**M**) Quantification of mRNA expression by quantitative RT-PCR in isolated E14 kidney organ cultures (L) or in dissected kidneys at different developmental stages (M). The experiments were repeated at least twice. *$P<0.005$, $^{\dagger}P<0.05$. (**N**) Comparison of gene expression between the kidney and the salivary glands. Analogous changes in gene expression were observed in these organs in *Cp2l1*$^{tra/tra}$ mice. Changes are indicated with arrows, and a battery of genes commonly expressed in the developmental programs of these organs is shown in color. Scale bars: 200 μm in A,C,D,G,I,K; 100 μm in B,E,F,H,J.

Table 3. Summary of gene expression in the developing kidney

Gene	Stage	*Cp2l1*$^{+/tra}$	*Cp2l1*$^{tra/tra}$	*P*
Atp6b1	E13	ND	ND	
	E15	9.41±3.84	0.28±0.16	<0.005
	E18	104.48±12.76	10.80±4.26	<0.001
	P0	100±26.02	8.62±0.88	<0.005
pendrin	E13	ND	ND	
	E15	2.93±2.12	0.14±0.00	<0.001
	E18	44.40±14.40	0.32±0.00	<0.001
	P0	100±25.54	2.98±1.79	<0.001
keratin 7	E13	7.10±0.06	5.00±1.55	0.06
	E15	25.35±0.00	12.37±2.60	<0.01
	E18	83.00±0.00	51.6±6.69	<0.001
	P0	100±0.01	58.72±7.36	0.01
Scnn1b	E13	ND	ND	
	E15	25.32±6.43	18.40±3.21	0.12
	E18	82.23±5.56	59.39±12.9	<0.05
	P0	100±11.72	65.62±5.76	0.01
Aqp2	E13	ND	ND	
	E15	2.97±1.73	1.34±0.64	0.17
	E18	69.01±22.82	51.77±11.11	0.23
	P0	100±33.50	77.65±9.49	0.32
keratin 19	E13	6.79±0.97	6.90±2.37	0.93
	E15	52.84±6.95	57.15±11.44	0.54
	E18	88.01±10.19	160.37±14.83	<0.001
	P0	100±25.52	176.40±73.74	<0.005
Gk-6	E13	ND	ND	
	E15	3.42±0.82	1.45±0.44	0.005
	E18	105.58±18.15	13.16±5.69	<0.001
	P0	100±15.72	14.16±2.52	<0.001
Clcnkb	E13	ND	ND	
	E15	4.52±2.10	ND	
	E18	66.58±14.74	17.18±5.39	<0.001
	P0	100±16.37	21.09±3.60	<0.001

Relative expression levels (mean±s.d., *n*=4-9) were normalized to cyclophilin D.
ND, not detected.

unchanged in *Cp2l1*$^{tra/tra}$ mice (Fig. 5C-E) (Dressler et al., 1990; Fushimi et al., 1993). Thus, the expression of the markers specific for distinct regions of nephric tubules and the CD was normally detected in *Cp2l1*$^{tra/tra}$ mice.

Despite expression of regional markers of the nephric tubules and CD in *Cp2l1*$^{tra/tra}$ mice, we found that they have abnormalities in the maturation of renal tubules. The CD is composed of type A intercalated cells (ICs), type B (non-A) ICs and principle cells (Kim et al., 1999). Type A ICs mediate proton secretion into and bicarbonate resorption from the lumen, and type B (non-A) ICs mediate bicarbonate secretion. The expression of *Atp6b1* (*Atp6v1b1* – Mouse Genome Informatics), which encodes the B1 subunit of vacuolar H^+-ATPase and mediates proton secretion at the apical membrane of type A ICs (Finberg et al., 2005), was lost in *Cp2l1*$^{tra/tra}$ mice at birth (Fig. 6A). Likewise, expression of *Slc4a1*, which encodes anion exchanger 1 and is a marker gene for type A ICs (Southgate et al., 1996), and pendrin, which is a marker gene for type B (non-A) ICs (Kim et al., 2002; Royaux et al., 2001), was

Table 4. Analysis of plasma, saliva and urine in adult *Cp2l1* mutant mice

Analysis	Control (+/+ and +/*tra*)*	Homo (*tra*/*tra*)*	*P* (*t*-test)
Plasma Na^+ conc. (mEq/l)	152.1±5.4	148.6±7.4	
Plasma K^+ conc. (mEq/l)	4.0±0.4	3.6±0.8	
Plasma Cl^- conc. (mEq/l)	112.8±4.4	110.4±7.7	
Saliva Na^+ conc. (mEq/l)	83.0±4.9	177±2.0	*P*<0.001
Saliva K^+ conc. (mEq/l)	32.7±3.0	16.3±1.5	*P*<0.001
Saliva Cl^- conc. (mEq/l)	85.0±7.6	160±3.4	*P*<0.001
Saliva volume (μl/15 min.g)	7.0±4.0	8.3±3.6	
Saliva flow rate (0-5 min) (μl/min)	19±13.8	14±3.46	
Urine Na^+ conc. (mEq/l)	127.5±35.6	109.5±6.3	
Net Na^+ excretion/day.g	7.0±2.0	12.1±4.1	*P*<0.05
Urine K^+ conc. (mEq/l)	182.5±42.6	135.1±22.2	
Net K^+ excretion/day.g	10.1±2.9	14.5±4.1	*P*<0.05
Urine Cl^- conc. (mEq/l)	203±68.2	193.8±55.3	
Net Cl^- excretion/day.g	11.2±4.4	20.6±7.8	*P*<0.05
Net urine volume (ml/day.g)	0.057±0.015	0.11±0.034	*P*<0.005
Body weight (g)	31.1±2.55	29.3±2.29	

*Mean±s.d. (*n*=6-10).

absent in *Cp2l1*$^{tra/tra}$ mice (Fig. 6B,M and data not shown). These abnormalities were evident from E15, before a time when the expression of these two genes is drastically increased during normal development (Fig. 6M and Table 3). These results showed that differentiation of ICs was defective in the *Cp2l1*$^{tra/tra}$ mice.

Furthermore, other aspects of maturation of the CD and distal tubules were disturbed in the *Cp2l1*$^{tra/tra}$ mice. Whereas keratin 7 was expressed throughout the CD system in normal embryos, its expression in the CD was very low or absent at E18 in the mutants (Fig. 6C,E,M). This reduced expression was partially recovered at birth in the medullary CD, but loss of keratin 7 expression was persistent in the cortical CD (Fig. 6D,F). Likewise, the expression of *Scnn1b* in the CD, as determined by quantitative RT-PCR, was also significantly decreased (Fig. 6M). By contrast, from E18, keratin 19 expression in the medullary CD was higher in the mutants than in normal mice (Fig. 6G,M).

Differentiation of not only the CD but also the distal tubules was also disrupted in *Cp2l1*$^{tra/tra}$ mice. The expression of *Gk-6* and *Fxyd2c*, which are expressed in newly formed DCT and CNT (Fig. 6H) and encode a serine protease and Na^+,K^+-ATPase γ-subunit variant c, respectively, was diminished in the mutants (Fig. 6I,J,M). Furthermore, the expression of *Clcnkb*, which encodes a chloride channel and is expressed in TAL and DCT (Kobayashi et al., 2001), was severely reduced in the mutants (Fig. 6K,M).

The CD and distal tubules are crucial compartments for the tight regulation of fluid, mineral and acid-base homeostasis, and gene expression in these tissues is regulated by physiological changes (Reilly and Ellison, 2000). Therefore, the observed phenotype might be an indirect consequence of possible physiological changes occurring in the mutants, such as altered fluid flow and composition caused by the loss of CP2L1. To see whether this is the case, we examined the development of kidney in culture explants, wherein the lack of a blood supply precludes the influence of physiological changes. The kidneys were isolated from E14 embryos, cultured for 2 days and subjected to gene expression analysis. The observed changes in gene expression were similar to those observed in embryos. For instance, the expression of *Atp6b1*, keratin 7, *Scnn1b*, *Fxyd2c*, *Clcnkb* and *Gk-6* was significantly lower in explants from *Cp2l1*$^{tra/tra}$ mice than in wild-type mice, whereas the expression of *Aqp2* did not differ significantly (Fig. 6L). This strongly suggested that the abnormal gene expression in the mutants was not a secondary consequence of a physiological abnormality. Taken together, the results indicate that CP2L1 is required for proper maturation of the CD and distal tubules during development of the kidney.

Abnormal composition of saliva and urine of *Cp2l1*$^{tra/tra}$ mice

To examine whether the defects observed in perinatal and postnatal developmental stages actually lead to functional abnormalities of these organs in adulthood, we measured the volume and electrolyte composition of saliva and urine collected from the surviving mutants (Table 4). Saliva is primarily generated in the acini and subsequently modified in the duct by resorption of electrolytes (Young et al., 1987). *Cp2l1*$^{tra/tra}$ mice secreted the same volume as control *Cp2l1*$^{+/+}$ or *Cp2l1*$^{+/tra}$ mice. Thus, the function of the acinus in *Cp2l1*$^{tra/tra}$ mice appeared normal, which is consistent with our previous observations indicating normal acinus formation. Sodium and chloride concentrations were much higher, and the potassium concentration was significantly lower, in the saliva from both male and female mutants than in saliva from normal mice. By contrast, the concentrations of these ions in plasma were not significantly different in mutants and normal mice. In consistent with the abnormal electrolyte composition of saliva in adult *Cp2l1*$^{tra/tra}$ mice, the expression of *Scnn1b* was not detected in the SMG duct of these mice (data not shown). Thus, modification of the electrolyte composition in saliva, a physiological function of the ducts, appeared to be abnormal in *Cp2l1*$^{tra/tra}$ mice.

Likewise, *Cp2l1*$^{tra/tra}$ mice showed variations in urine output in surviving adults. Urine is primarily filtrated through the glomerulus and subsequently modified through the renal tubules and ducts by resorption and secretion of minerals and water. *Cp2l1*$^{tra/tra}$ mice exhibit mild polyurine and discharge of more electrolytes (see total urine volume and net secretion of each electrolyte in Table 4). At least a part of this abnormality appeared to be due to insufficient maturation of the distal tubules and CD in *Cp2l1*$^{tra/tra}$ mice. However, we cannot exclude the possibility that these abnormalities are due to an inability to concentrate urine in the mutant kidney, which exhibits structural abnormalities and kidney hypoplasia in adults (Yamaguchi et al., 2005). In any case, these results showed that both the salivary gland and kidney require CP2L1 for their proper physiological function as intact organs.

DISCUSSION

Here, we showed that CP2L1 is required for proper maturation of the duct of the salivary gland. Although a surface structure composed of acini and ducts appeared to be properly established in the SMG of *Cp2l1*$^{tra/tra}$ mice, functional maturation of the duct, which is specified by the expression of genes regulating cellular physiology, such as *Scnn1b*, *β-NGF* and *Gk-6*, was disrupted from embryonic stages to adulthood. Along with the abnormal gene expression, the apical structure of duct cells was not well developed and the lumen was dilated. Given that the duct is a site for modification of saliva, it is likely that the abnormal electrolyte composition of saliva in the mutant mice is the consequence of the defects in maturation.

Cp2l1 was also required for duct maturation in the kidney. The tubule architecture and regionalization monitored by expression of marker genes specific for distinct regions of nephrons appeared normal in *Cp2l1*$^{tra/tra}$ mice, but gene expression characteristic of CD and distal tubule maturation was abnormal in the mutants. In particular, the expression of *Atp6b1*, *Slc4a1* and pendrin, which are typical markers of differentiated ICs, was not detected during any of the embryonic stages, indicating that generation of ICs was severely defective in *Cp2l1*$^{tra/tra}$ mice (Fig. 6M and Table 3). The expression of keratin 7 and *Scnn1b*, which is elevated during maturation of the CD, was also reduced in *Cp2l1*$^{tra/tra}$ mice. Because the reduced expression of these genes recovered to the normal level after birth, at least some aspects of CD development appear to be delayed in the mutants. Likewise, it appeared that maturation of distal tubules (TAL, DCT and CNT) was also disrupted in *Cp2l1*$^{tra/tra}$ mice, because they did not express *Clcnkb*, *Gk-6* or *Fxyd2c*. Importantly, abnormal expression of these genes was also detected in cultured mutant kidneys, indicating that defective gene expression in the mutant kidney was not due to changes in the external environment caused by the loss of *Cp2l1*. Rather, it appears that the defective maturation of nephric tubules leads to insufficient renal function and frequent death within a few weeks after birth.

The identification of a gene essential for the maturation of the exocrine ducts and kidney should help to elucidate their underlying molecular mechanisms. Duct maturation includes both duct formation and the acquisition of physiological function. Because CP2L1 is a transcriptional regulator, genes with expression is directly or indirectly regulated by this factor may be involved in these processes. In *Cp2l1*-deficient embryos, the expression of genes

involved in the physiological function of the ducts was reduced; for example *Cp2l1*-deficient mice displayed reduced expression of *Scnn1b*, *Fxyd2 and Atp6b1*, which encode the β-subunit of the epithelial sodium channel (Nakai et al., 2003; Schmitt et al., 1999), a possible regulatory subunit of Na^+,K^+-ATPase (Arystarkhova et al., 2002; Jones et al., 2001; Jones et al., 2005), and the B1-subunit of vacuolar ATPase (Finberg et al., 2005), respectively. In addition to the genes directly involved in physiological function, we found that the expression of keratin genes was also abnormal in the ducts of the mutants. Keratin 7 is a type 2 intermediate filament protein distributed broadly in, and a hallmark of, glandular ducts (Smith et al., 2002). The apical localization of keratin 7 (Fig. 1C) may be involved in morphological differentiation in luminal cells because a cytoskeleton-rich structure in the apical side of the cells did not develop sufficiently in the salivary duct of *Cp2l1*$^{tra/tra}$ mice, which lack keratin 7 expression. Given that keratin 8, a type 2 basic keratin filament like keratin 7, is essential for the proper intracellular trafficking of membrane channels and transporter proteins in colon cells (Toivola et al., 2004), it is possible that keratin 7 contributes to proper glandular duct formation by regulating intracellular trafficking. Likewise, the expression of keratin 19 (Lussier et al., 1990), which encodes a type 1 acidic keratin filament, was not properly reduced during development but remained at a high level in the ducts of *Cp2l1*$^{tra/tra}$ mice. Together, these results indicate that CP2L1 participates in establishing the function of ducts by coordinating the expression of several genes that are involved in physiological function and generate the appropriate cellular architecture.

Different organs developing from distinct lineages often show similarities in their morphogenetic processes (Davies, 2002; Hogan and Kolodziej, 2002). This is also true for their physiological properties. The exocrine glands and kidney share common basal structures and function; in the proximal part of the glands, secretions into the lumen are generated, and in a distal part, the duct, the primary fluid flowing through its lumen is modified by absorption and secretion. Hence, it is thought that there is a common molecular basis for the generation of the structural and functional similarities in the exocrine glands and kidney. *Cp2l1* was specifically expressed during the development of the ducts in many exocrine glands, including ducts in the salivary, nasal, lachrymal, sweat and mammary glands as well as in the kidney. In this study, we revealed that CP2L1 is essential for proper maturation of the salivary ducts and the kidney. Interestingly, we found that CP2L1 is required for the expression of a set of genes, including *Fxyd2*, *Gk-6*, *Scnn1b* and keratin 7, which are expressed commonly in the developing ducts of the salivary gland and kidney (Fig. 6N). In addition, the expression of keratin 7 and *Gk-6* was reduced in the nasal gland of *Cp2l1*-deficient mice (Fig. 3E and data not shown). These lines of evidence suggest that a *Cp2l1*-dependent gene expression program constitutes a molecular mechanism that generates the analogous properties of the ducts in exocrine glands and kidney. Combination of higher resolution analysis at a single-cell level and exhaustive and comparative analysis of different organs using DNA microarrays is needed to determine the validity of this hypothesis.

We thank H. Watanabe, T. Hiroe, N. Inoue, K. Irie, N. Takeda, M. Sasaki, A. Ohbayashi, and N. Ohbayashi for their technical support and S. Sasaki, J.Sakiyama, M. Wada, K. Ono, M. Takeichi and all members of S.T. Labs for their helpful advice. We also thank M. Karasawa, H. Takebayashi, S. Nakai, P. Gruss and S. Yoshida for providing materials. This work was supported by a grant-in-aid for scientific research from the Ministry of Education, Science, Culture, and Sports of Japan and the Uehara Memorial Foundation (to S.T.).

Supplementary material

Supplementary material for this article is available at http://dev.biologists.org/cgi/content/full/133/23/4737/DC1

References

Arystarkhova, E., Wetzel, R. K. and Sweadner, K. J. (2002). Distribution and oligomeric association of splice forms of Na(+)-K(+)-ATPase regulatory gamma-subunit in rat kidney. *Am. J. Physiol. Renal Physiol.* **282**, F393-F407.

Bray, S. J. and Kafatos, F. C. (1991). Developmental function of Elf-1: an essential transcription factor during embryogenesis in Drosophila. *Genes Dev.* **5**, 1672-1683.

Davies, J. A. (2002). Do different branching epithelia use a conserved developmental mechanism? *BioEssays* **24**, 937-948.

Ding, L., Takebayashi, H., Watanabe, K., Ohtsuki, T., Tanaka, K. F., Nabeshima, Y., Chisaka, O., Ikenaka, K. and Ono, K. (2005). Short-term lineage analysis of dorsally derived Olig3 cells in the developing spinal cord. *Dev. Dyn.* **234**, 622-632.

Dressler, G. R., Deutsch, U., Chowdhury, K., Nornes, H. O. and Gruss, P. (1990). Pax2, a new murine paired-box-containing gene and its expression in the developing excretory system. *Development* **109**, 787-795.

Finberg, K. E., Wagner, C. A., Bailey, M. A., Paunescu, T. G., Breton, S., Brown, D., Giebisch, G., Geibel, J. P. and Lifton, R. P. (2005). The B1-subunit of the H(+) ATPase is required for maximal urinary acidification. *Proc. Natl. Acad. Sci. USA* **102**, 13616-13621.

Fushimi, K., Uchida, S., Hara, Y., Hirata, Y., Marumo, F. and Sasaki, S. (1993). Cloning and expression of apical membrane water channel of rat kidney collecting tubule. *Nature* **361**, 549-552.

Gresik, E. W. and Barka, T. (1980). Precocious development of granular convoluted tubules in the mouse submandibular gland induced by thyroxine or by thyroxine and testosterone. *Am. J. Anat.* **159**, 177-185.

Grieshammer, U., Cebrian, C., Ilagan, R., Meyers, E., Herzlinger, D. and Martin, G. R. (2005). FGF8 is required for cell survival at distinct stages of nephrogenesis and for regulation of gene expression in nascent nephrons. *Development* **132**, 3847-3857.

Hemphala, J., Uv, A., Cantera, R., Bray, S. and Samakovlis, C. (2003). Grainy head controls apical membrane growth and tube elongation in response to Branchless/FGF signalling. *Development* **130**, 249-258.

Hogan, B. L. and Kolodziej, P. A. (2002). Organogenesis: molecular mechanisms of tubulogenesis. *Nat. Rev. Genet.* **3**, 513-523.

Huang, N. and Miller, W. L. (2000). Cloning of factors related to HIV-inducible LBP proteins that regulate steroidogenic factor-1-independent human placental transcription of the cholesterol side-chain cleavage enzyme, P450scc. *J. Biol. Chem.* **275**, 2852-2858.

Jones, D. H., Golding, M. C., Barr, K. J., Fong, G. H. and Kidder, G. M. (2001). The mouse Na+-K+-ATPase gamma-subunit gene (Fxyd2) encodes three developmentally regulated transcripts. *Physiol. Genom.* **6**, 129-135.

Jones, D. H., Li, T. Y., Arystarkhova, E., Barr, K. J., Wetzel, R. K., Peng, J., Markham, K., Sweadner, K. J., Fong, G. H. and Kidder, G. M. (2005). Na,K-ATPase from mice lacking the gamma subunit (FXYD2) exhibits altered Na+ affinity and decreased thermal stability. *J. Biol. Chem.* **280**, 19003-19011.

Kim, J., Kim, Y. H., Cha, J. H., Tisher, C. C. and Madsen, K. M. (1999). Intercalated cell subtypes in connecting tubule and cortical collecting duct of rat and mouse. *J. Am. Soc. Nephrol.* **10**, 1-12.

Kim, Y. H., Kwon, T. H., Frische, S., Kim, J., Tisher, C. C., Madsen, K. M. and Nielsen, S. (2002). Immunocytochemical localization of pendrin in intercalated cell subtypes in rat and mouse kidney. *Am. J. Physiol. Renal. Physiol.* **283**, F744-F754.

Kobayashi, K., Uchida, S., Mizutani, S., Sasaki, S. and Marumo, F. (2001). Intrarenal and cellular localization of CLC-K2 protein in the mouse kidney. *J. Am. Soc. Nephrol.* **12**, 1327-1334.

Kudryavtseva, E. I., Sugihara, T. M., Wang, N., Lasso, R. J., Gudnason, J. F., Lipkin, S. M. and Andersen, B. (2003). Identification and characterization of Grainyhead-like epithelial transactivator (GET-1), a novel mammalian Grainyhead-like factor. *Dev. Dyn.* **226**, 604-617.

Lim, L. C., Swendeman, S. L. and Sheffery, M. (1992). Molecular cloning of the alpha-globin transcription factor CP2. *Mol. Cell. Biol.* **12**, 828-835.

Lussier, M., Filion, M., Compton, J. G., Nadeau, J. H., Lapointe, L. and Royal, A. (1990). The mouse keratin 19-encoding gene: sequence, structure and chromosomal assignment. *Gene* **95**, 203-213.

Mace, K. A., Pearson, J. C. and McGinnis, W. (2005). An epidermal barrier wound repair pathway in Drosophila is mediated by grainy head. *Science* **308**, 381-385.

Muroyama, Y., Fujihara, M., Ikeya, M., Kondoh, H. and Takada, S. (2002). Wnt signaling plays an essential role in neuronal specification of the dorsal spinal cord. *Genes Dev.* **16**, 548-553.

Nakai, S., Sugitani, Y., Sato, H., Ito, S., Miura, Y., Ogawa, M., Nishi, M., Jishage, K., Minowa, O. and Noda, T. (2003). Crucial roles of Brn1 in distal tubule formation and function in mouse kidney. *Development* **130**, 4751-4759.

Neiss, W. F. (1982). Histogenesis of the loop of Henle in the rat kidney. *Anat. Embryol.* **164**, 315-330.

Parekh, V., McEwen, A., Barbour, V., Takahashi, Y., Rehg, J. E., Jane, S. M. and Cunningham, J. M. (2004). Defective extraembryonic angiogenesis in mice lacking LBP-1a, a member of the grainyhead family of transcription factors. *Mol. Cell. Biol.* **24**, 7113-7129.

Penschow, J. D., Drinkwater, C. C., Haralambidis, J. and Coghlan, J. P. (1991). Sites of expression and induction of glandular kallikrein gene expression in mice. *Mol. Cell. Endocrinol.* **81**, 135-146.

Reilly, R. F. and Ellison, D. H. (2000). Mammalian distal tubule: physiology, pathophysiology, and molecular anatomy. *Physiol. Rev.* **80**, 277-313.

Rodda, S., Sharma, S., Scherer, M., Chapman, G. and Rathjen, P. (2001). CRTR-1, a developmentally regulated transcriptional repressor related to the CP2 family of transcription factors. *J. Biol. Chem.* **276**, 3324-3332.

Royaux, I. E., Wall, S. M., Karniski, L. P., Everett, L. A., Suzuki, K., Knepper, M. A. and Green, E. D. (2001). Pendrin, encoded by the Pendred syndrome gene, resides in the apical region of renal intercalated cells and mediates bicarbonate secretion. *Proc. Natl. Acad. Sci. USA* **98**, 4221-4226.

Schmitt, R., Ellison, D. H., Farman, N., Rossier, B. C., Reilly, R. F., Reeves, W. B., Oberbaumer, I., Tapp, R. and Bachmann, S. (1999). Developmental expression of sodium entry pathways in rat nephron. *Am. J. Physiol.* **276**, F367-F381.

Smith, F. J., Porter, R. M., Corden, L. D., Lunny, D. P., Lane, E. B. and McLean, W. H. (2002). Cloning of human, murine, and marsupial keratin 7 and a survey of K7 expression in the mouse. *Biochem. Biophys. Res. Commun.* **297**, 818-827.

Southgate, C. D., Chishti, A. H., Mitchell, B., Yi, S. J. and Palek, J. (1996). Targeted disruption of the murine erythroid band 3 gene results in spherocytosis and severe haemolytic anaemia despite a normal membrane skeleton. *Nat. Genet.* **14**, 227-230.

Sueyoshi, T., Kobayashi, R., Nishio, K., Aida, K., Moore, R., Wada, T., Handa, H. and Negishi, M. (1995). A nuclear factor (NF2d9) that binds to the male-specific P450 (Cyp 2d-9) gene in mouse liver. *Mol. Cell. Biol.* **15**, 4158-4166.

Tandler, B. (1993). Structure of the duct system in mammalian major salivary glands. *Microsc. Res. Tech.* **26**, 57-74.

Tao, J., Kuliyev, E., Wang, X., Li, X., Wilanowski, T., Jane, S. M., Mead, P. E. and Cunningham, J. M. (2005). BMP4-dependent expression of Xenopus Grainyhead-like 1 is essential for epidermal differentiation. *Development* **132**, 1021-1034.

Ting, S. B., Wilanowski, T., Auden, A., Hall, M., Voss, A. K., Thomas, T., Parekh, V., Cunningham, J. M. and Jane, S. M. (2003). Inositol- and folate-resistant neural tube defects in mice lacking the epithelial-specific factor Grhl-3. *Nat. Med.* **9**, 1513-1519.

Ting, S. B., Caddy, J., Hislop, N., Wilanowski, T., Auden, A., Zhao, L. L., Ellis, S., Kaur, P., Uchida, Y., Holleran, W. M. et al. (2005). A homolog of Drosophila grainy head is essential for epidermal integrity in mice. *Science* **308**, 411-413.

Toivola, D. M., Krishnan, S., Binder, H. J., Singh, S. K. and Omary, M. B. (2004). Keratins modulate colonocyte electrolyte transport via protein mistargeting. *J. Cell Biol.* **164**, 911-921.

Venkatesan, K., McManus, H. R., Mello, C. C., Smith, T. F. and Hansen, U. (2003). Functional conservation between members of an ancient duplicated transcription factor family, LSF/Grainyhead. *Nucleic Acids Res.* **31**, 4304-4316.

Wilanowski, T., Tuckfield, A., Cerruti, L., O'Connell, S., Saint, R., Parekh, V., Tao, J., Cunningham, J. M. and Jane, S. M. (2002). A highly conserved novel family of mammalian developmental transcription factors related to Drosophila grainyhead. *Mech. Dev.* **114**, 37-50.

Yamaguchi, Y., Ogura, S., Ishida, M., Karasawa, M. and Takada, S. (2005). Gene trap screening as an effective approach for identification of Wnt-responsive genes in the mouse embryo. *Dev. Dyn.* **233**, 484-495.

Yoon, J. B., Li, G. and Roeder, R. G. (1994). Characterization of a family of related cellular transcription factors which can modulate human immunodeficiency virus type 1 transcription in vitro. *Mol. Cell. Biol.* **14**, 1776-1785.

Yoshida, S., Ohbo, K., Takakura, A., Takebayashi, H., Okada, T., Abe, K. and Nabeshima, Y. (2001). Sgn1, a basic helix-loop-helix transcription factor delineates the salivary gland duct cell lineage in mice. *Dev. Biol.* **240**, 517-530.

Young, J. A., Cook, D. I., van Lennep, E. W. and Roberts, M. (1987). Secretion by the major salivary glands. In *Physiology of the Gastrointestinal Tract* (2nd edn) (ed. L. R. Johnson), pp. 773-815. New York: Raven Press.